Design and Simulation of Contour mode MEMS Resonator on Si for Power Converters

Abusaleh M. Imtiaz and Faisal H. Khan
Power Electronics and Automation Research Lab (PEARL)
Dept. of Electrical and Computer Engineering,
Univ. of Utah, Salt Lake City, USA
as.imtiaz@utah.edu, faisal.khan@utah.edu

Abstract—**Microelectromechanical systems (MEMS) resonators on Si have the potential to replace the discrete passive components in a power converter. These devices not only can reduce the size and weight of the converter but also can facilitate the implementation of power converter on a chip. In this paper, a contour mode MEMS resonator has been presented that can achieve resonant frequency in the range of several MHz, and the operating principles of the device have been discussed in detail. This device was simulated in COMSOL Multiphysics, and a resonant converter has been simulated in PSIM to harvest energy from a thermo electric generator. The equivalent electrical model of the MEMS resonator was incorporated into that circuit validating the feasibility of using MEMS resonator in power conversion systems. Detailed fabrication process of the device has been presented and implemented at University of Utah's Nanofab. Initial experimental characteristics of the resonator have been included in the paper.**

I. INTRODUCTION

Power converters have been traditionally constructed from magnetic components and have not encountered miniaturization and integration until recently. Acoustic rather than inductive power transfer can be employed in power converters to further miniaturize components, and acoustic coupling can be achieved through piezoelectric materials. In this regard, MEMS devices using acoustic coupling such as film bulk acoustic resonator (FBAR) can be used in power converters [1]. This MEMS resonator is compatible with conventional CMOS process and can easily be integrated.

A piezoelectric resonator is an elastic body consisting of a piezoelectric material that can be excited to cause vibration when an alternating electric field with resonating frequency is applied to it. The mechanical vibration in the neighborhood of the resonant frequency depends on the inertia, elastic compliance, and stiffness of the resonant element, and those correspond to inductance, capacitance and resistance of an equivalent electronic network. The equivalent electrical model of FBAR is shown in Fig. 1, and this model is known as Butterworth-Van Dyke (BVD) model [1], [2]. This resonator can be used to replace the discrete L-C resonant tank used inside resonant converters [1]. Besides achieving higher quality factor (QF) compared to discrete L-C resonators [4], FBAR can offer superior electromagnetic interference (EMI) performance [1]. The resonant frequency of these devices are primarily determined by the thickness of the piezoelectric film deposited by standard CMOS processes such as sputtering or chemical vapor deposition (CVD) according to

$$v = \sqrt{\frac{E}{p}}$$

and $f = \frac{v}{2d}$,

where E, p, d, and V are the elastic constant, density, thickness, and acoustic velocity of the film and f is the resonant frequency of the FBAR [3]. In order to achieve resonant frequency in the range of several MHz, the thickness of the film should be in the range of tens of micrometers. This is quite difficult to achieve in CMOS process due to long deposition time and higher stress imposed on the thick film. In order to solve this issue, a contour mode MEMS resonator has been presented in this paper. The operating principles of the resonator and fabrication process to integrate this device with CMOS have been included in the paper as well. COMSOL Multiphysics has been used to simulate this device, and the simulation results have been included in the paper. Details of the fabrication process as implemented at University of Utah's Nanofab have been presented. The fabricated devices were tested and these initial results are included in the paper.

Besides MEMS resonator on Si, piezoelectric materials can be utilized to construct miniature piezoelectric transformer. These transformers utilizes electromechanical coupling between the primary and secondary piezoelectric elements for step-up or step-down voltage conversion. In addition to the aforementioned advantages, piezoelectric transformer can

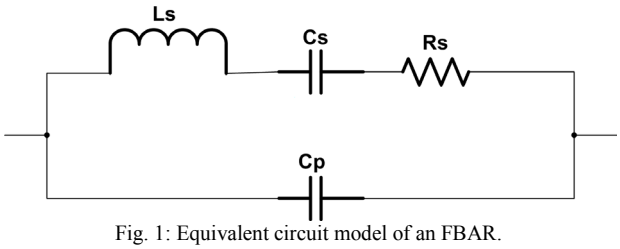

Fig. 1: Equivalent circuit model of an FBAR.

978-1-4673-4916-1/13/$31.00 ©2013 IEEE

save weight and space compared to conventional transformers. Moreover, these devices are inflammable and bio-friendly. In recent days, the use of micro-watt thermoelectric generator (TEG) allows us to convert body heat into electricity for powering implantable devices. The voltage produced by these devices is in the range of 25-50 mV [5]. In order to power the CMOS ICs using TEG, a very high voltage boosting is necessary (the supply voltages required by the ICs are higher than 1 V). Complex control circuits have been proposed to achieve this boosting operation incorporating a boost converter [6], [7]. MEMS resonator based resonant converter would be an excellent choice for this application because piezoelectric transformers can easily achieve very high voltage step up (50-80) and they are compatible with functional magnetic resonance imaging (FMRI) to study brain activity. Therefore, piezoelectric transformer based resonant converter has been proposed for TEG energy harvesting application at the last part of the paper, and PSIM simulation results have been included to prove this concept.

II. Basic Principles of Contour Mode Piezoelectric Resonator

Piezoelectricity - a physical phenomenon, discovered by the Curie brothers, is a linear interaction between electrical and mechanical domains happening within a single elastic body. The behavior of piezoelectric elements can be described using the two fundamental equations of piezoelectricity [8]-[10]

$$S = s^E.T + d_t.E \quad (1)$$

and $D = d.T + \varepsilon^T.E$ (2)

where, S is the mechanical strain, T is the mechanical stress, E is the electric field, D is the electric displacement, d is piezoelectric constant s^E is elastic compliance at constant electric field, and ε^T is permittivity at constant stress. According to Eq. (1), applying an electric field on a piezoelectric material results in a mechanical strain S (actuator operation). Eq. (2) describes, with an applied mechanical stress T, an electric displacement is induced on the electric plates of the piezoelectric material (transducer action). Typically, the electrode plates are along the direction of axis 3 (Fig. 2), therefore, the electric field, E, and electric displacement, D, are in the direction of axis 3 (the non-zero component of the electric field is E_3). The fundamental matrix of piezoelectric constants for a typical piezoelectric material is as following:

$$d_t = d_{transpose} = \begin{matrix} 0 & 0 & d_{13} \\ 0 & 0 & d_{23} \\ 0 & 0 & d_{33} \\ 0 & d_{42} & 0 \\ d_{51} & 0 & 0 \\ 0 & 0 & 0 \end{matrix}$$

A piezoelectric resonator could be designed to resonate in thickness mode or in the contour mode, and the former mode (by means of d_{33} piezoelectric constant) is exploited in FBAR. For contour mode, d_{31} piezoelectric constant is utilized, and strain S_{11} can be achieved by applying electric field across the thickness of the film according to:

$S_{11} = d_{13}E_3$ (from (1)).

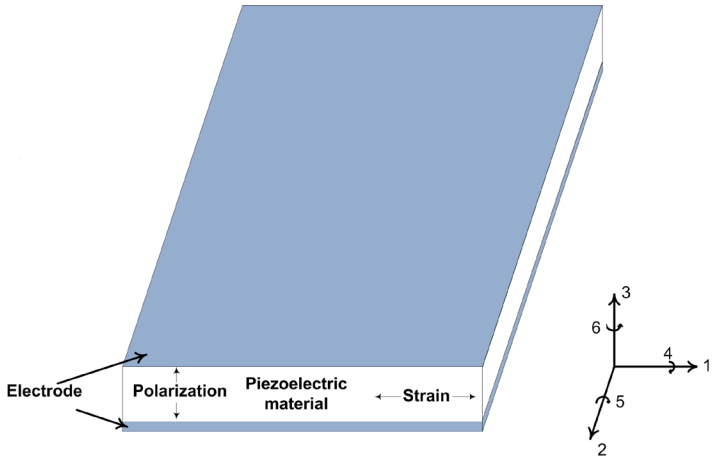

Fig. 2: Contour mode Piezoelectric resonator. 1- X axis, 2- Y axis, 3-axis, 4- sheer around x, 5- sheer around y and 6- sheer around z .

III. Proposed Device

Based on the above operating principles, a schematic of the proposed contour mode piezoelectric resonator on Si is shown in Fig. 3. In this structure, the thin piezoelectric film (AlN) is deposited directly on top of the Si substrate. Thin film piezoelectric on substrate (TPoS) takes the advantage of the low damping coefficient of the Si substrate layer. Dissipation in a TPoS resonator comes from the mechanical

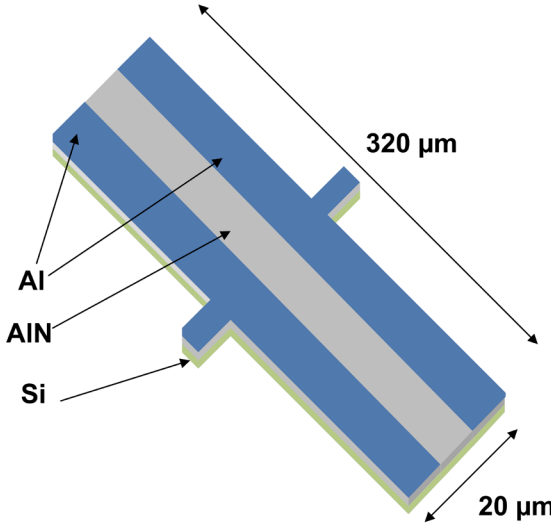

Fig. 3: Two port (three terminals) AlN contour mode rectangular plate MEMS resonator (figure is not drawn to the scale)

damping of each layer; the interfacial loss due to the mismatch between different layers (Si-AlN, AlN-Al) and electrical resistance of the electrodes. The Si substrate has been used as the bottom electrode in Fig. 3.

The advantages of using the substrate as the bottom electrode are twofold. First, the interface mismatch between the different layers has been reduced by eliminating the ground electrode. Normally, a typical MEMS resonator has three interfaces (Si-Al, Al-AlN, AlN-Al). However, the presented structure has two interfaces. Heavily doped Si substrate layer has the resistivity less than 0.001 Ω-cm, which makes it suitable for the ground electrode. Second, the damping coefficient of single-crystal Si is smaller compared to those of common piezoelectric materials and metals used as electrodes. These two factors contribute to lower loss of the presented device. In order to give proper support to the reasonably long device, SOI wafer has been considered. One common rule of MEMS device is that the length can be at most 80 times higher than its thickness. The top Si layer of the SOI wafer is 9 um, which is thick enough to support the 320 µm long device (Fig. 3).

Temperature coefficient of frequency (TCF) is an important parameter of the resonator once it is used for power conversion. Due to the losses incurred during the power conversion, the operating temperature of the device will change; this in turn will change the frequency of the device. Lower TCF is desirable in order to ensure the stability of the controller of the power converter incorporating a MEMS resonator. The TCF of a resonator can be determined from the temperature coefficient of elastic modulus (TCE) of each layer.

$$TCF \approx \sqrt{\frac{(1+TCE_i)E_i t_i + (1+TCE_j)E_j t_j + \ldots}{E_i t_i + E_j t_j + \ldots}} - 1 \qquad (3)$$

Where E and t are the elastic modulus and thickness of each layer respectively. Interestingly, the temperature coefficient of elastic modulus of Si can be reduced by increasing the doping level [11] [12]. Therefore, the highly doped Si substrate/ground electrode also contributes to the reduction of the temperature sensitivity of the frequency of resonance. The equivalent electrical model of the presented device at the neighborhood of the resonant frequency is shown in Fig. 4, which is suitable for series resonant converters.

IV. Proposed Fabrication Process

A four mask/lithography process has been proposed to fabricate the proposed resonator. The process starts with a SOI wafer having heavily doped Si device layer (the resistivity of the top Si layer is .001 ohm-cm with thickness of 9 µm). These special wafers were supplied by Ultrasil [15]. The bottom Si layer is 500 µm thick and the thickness of the buried oxide layer is 3 µm. Piezoelectric film with very good piezoelectric features is essential for piezoelectric resonator. A major issue related to fabrication of MEMS resonator is the deposition of highly polycrystalline and well oriented piezoelectric thin films in a repeatable manner. Lead Zirconate Titanate (PZT) is a widely used material for discrete resonators available in the commercial market. However, it suffers from compatibility issues with the semiconductor fabrication processes and not acceptable in most CMOS foundry. On the other hand, Thin AlN piezoelectric film can be deposited using conventional physical vapor deposition (PVD) tools using Al as the target material. Therefore, the resonator can be integrated easily with CMOS devices.

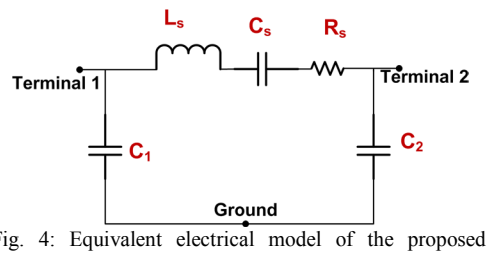

Fig. 4: Equivalent electrical model of the proposed resonator.

Table I gives a comparison of three piezoelectric materials – AlN, ZnO and PZT in terms of their properties. AlN has higher sound velocity which means for a given frequency, larger structure can be made with AlN. This gives an advantage for contour mode devices where the resonant frequency is mainly determined by the device length. The high dielectric breakdown voltage of AlN increases the voltage rating of the device fabricated from AlN. High resistivity of the film ensures good electrical isolation and lower dielectric constant means lower parasitic capacitance. This lower capacitance imposes less constraint to achieve zero voltage switching (ZVS). Therefore, AlN is chosen as the piezoelectric film of the proposed resonator.

500 nm thin AlN film was deposited using an Advanced Modular Sputtering (AMS) PVD tool (Figure 5a). A pure Al is used and Ar/N_2 forms the plasma for the deposition. This process was performed in an outside commercial foundry [16] in order to achieve highly c-axis (002) oriented AlN film with good polycrystalline structures. The uniformity of the film was verified by optically based film thickness measurement using Nanospec (AFT model 3000). The uniformity was better than 1% for a 100 mm (4 inch) wafer.

TABLE I: COMPARISON OF THE ELECTROMECHANICAL PROPERTIES OF THREE PIEZOELECTRIC MATERIALS

Property	AlN	ZnO	PZT
Sound velocity (km/s)	11.4	5.35	4.5
Permittivity (ε_3)	9	10	1000
Resistivity (Ωµm)	10^9	10^3	10^5
Dielectric strength (V/µm)	100	10	100
Piezoelectric coupling coefficient (K^2_{t31}) (%)	2.5	2.5	8-12

Dry etching is the preferred etching process for AlN. Cl_2 based inductively coupled plasma (ICP) reactive ion etching (RIE) is widely used for this purpose. Unfortunately, Utah Nanofab does not have this etching process available, and therefore, wet etching in warm phosphoric acid was adopted to etch AlN for this device. This etch rate depends strongly on the temperature of the acid. It is also difficult to achieve good uniformity over the entire wafer. Therefore, Careful inspection was necessary during wet etching of AlN, and efforts will be given to implement a dry etch process for AlN for future devices. Phosphoric acid at 100 ^oC etches the AlN layer and opens up the area for bottom electrode (Fig. 5b)

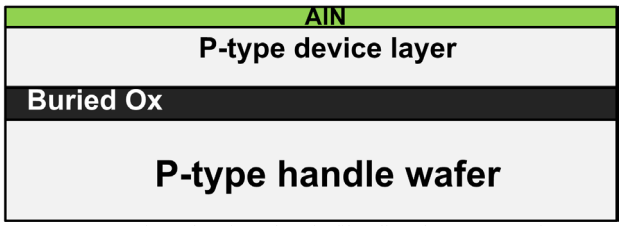

a: Sputtering AlN piezoelectric film directly on SOI wafer

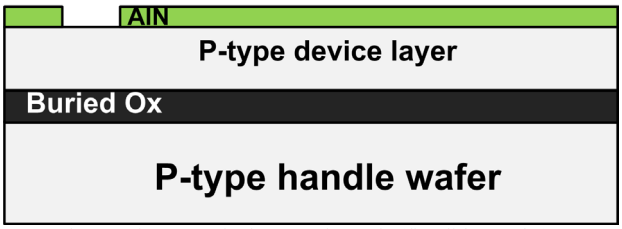

b: Opening areas for bottom electrode (first lithography)

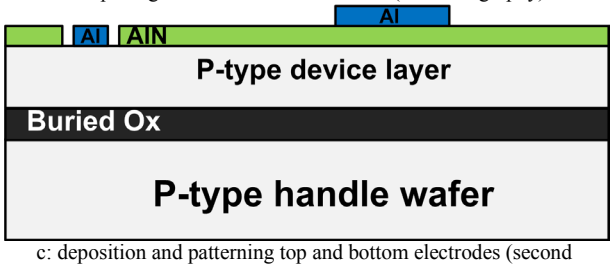

c: deposition and patterning top and bottom electrodes (second lithography)

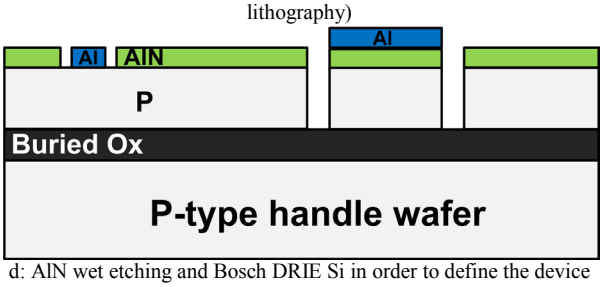

d: AlN wet etching and Bosch DRIE Si in order to define the device structure (third lithography)

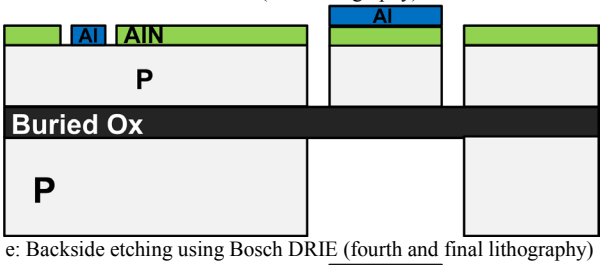

e: Backside etching using Bosch DRIE (fourth and final lithography)

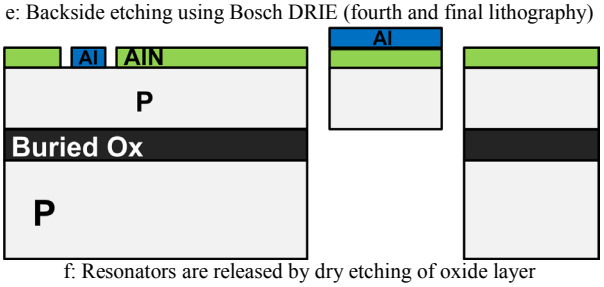

f: Resonators are released by dry etching of oxide layer

Fig. 5: Proposed fabrication process (figures are not drawn to the scale).

However, the structure needs to be released in order to resonate. This can be achieved by etching 3 µm buried oxide layer. In order to release the large dimensioned structures several hours of oxide etching in Buffered Oxide etchant (BOE) is necessary. BOE ($HF:NH_4OH$) is a strong etchant and attacks both Al and AlN. Therefore, it is not feasible to

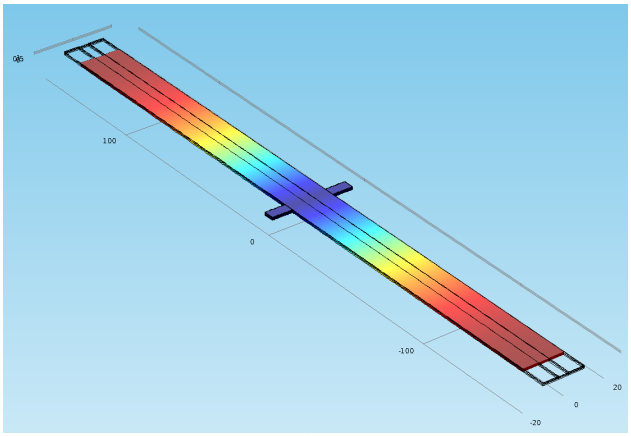
(a)

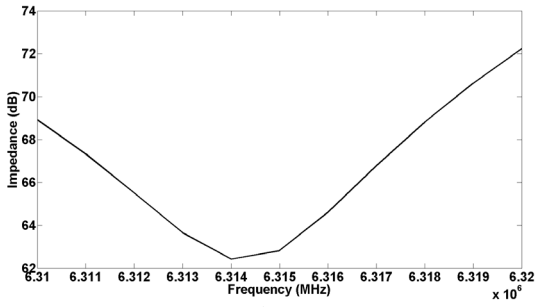

(b)

Fig. 6: COMSOL simulation results L = 320 µm, (a) there is a large strain along the length of the device at the frequency of resonance, (b) impedance response of the resonator which resembles impedance response of a series R-L-C circuit.

use BOE for a long duration as it will destroy the device structure, and for the same reason it was necessary to etch the device through the Sidebottom surface. The 500 µm handle Si layer was etched with the same Bosch DRIE process (SF_6:C_4F_8) to reach the buried oxide layer from the back side (Fig. 5e), and a careful back side lithography was necessary to achieve this. Dry etching using CF_4:O_2 plasma was used to etch the oxide layer and release the structure (Fig. 5f).

V. Simulation Results

The proposed MEMS resonator was simulated in COMSOL Multiphysics. The length of the device structure is the primary frequency determining factor according to

$$f = \frac{1}{2L}\sqrt{\frac{E_f}{\rho}} \quad (4),$$

E_f is the elastic modulus, ρ is the density of the piezo-electric material. The simulation results are shown in Fig. 6-7 for two different lengths of the device. The resonant frequency is approximately 6.314363 MHz (Fig. 6b) when L = 320 µm. The resonant frequency is doubled (12.6361 MHz) when L = 160 µm (Fig. 7b) according to (4). The frequency vs impedance characteristics shown in Fig. 6b and Fig. 7b span only 10 kHz demonstrating very high Q value of the resonators. The impedance is the minimum at the resonant frequency similar to a series R-L-C circuit (i.e a series R-L-C circuit also has the minimum impedance at the resonant frequency).

.

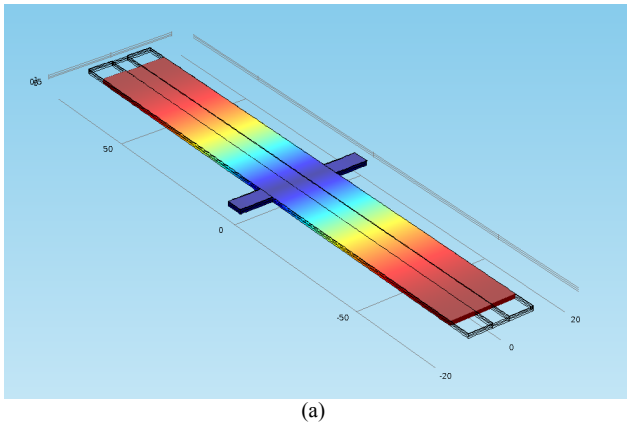

(a)

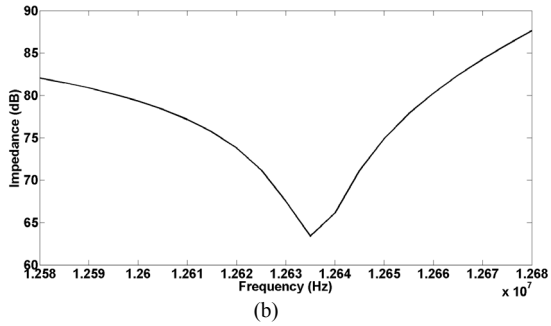

(b)

Fig. 7: COMSOL simulation results L = 160 µm, (a) there is a large strain along the length of the device at the frequency of resonance, (b) impedance response of the resonator which resembles impedance response of a series R-L-C circuit.

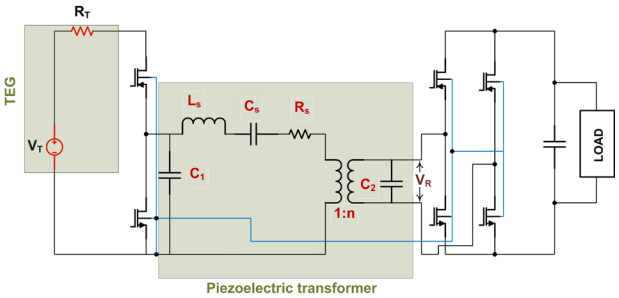

Fig. 8: Piezoelectric transformer based resonant converter for TEG applications

VI. Application of Contour Mode Piezoelectric Resonator

The contour mode piezoelectric resonator discussed in the previous section can be extended to build piezoelectric transformers (PZT) [13]. Fig. 8 shows a series resonant converter for TEG incorporating a PZT, and the TEG can be modeled as a voltage source with a resistance in series [5]-[7]. This circuit was simulated in PSIM 9, and the equivalent electrical model of a PZT with parameters from a commercial device [14] was used in the simulation. The simulation results are shown in Fig. 9.

VII. Exerimental Results/Device Characterization

Developing a process takes significant amount of time. The process described in section IV has been implemented only once to date. Therefore, the etch duration, film thickness,

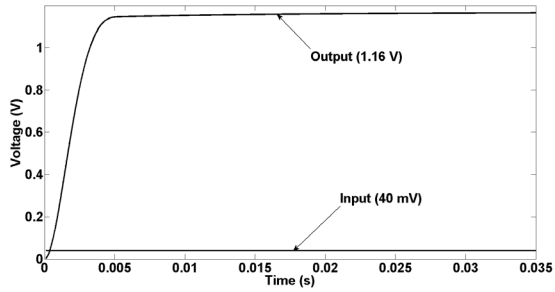

(a)

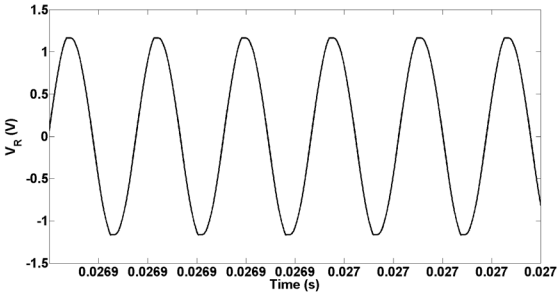

(b)

Fig. 9 (a) the input and output voltages of the converter. The high voltage boosting is possible due to the high step up ratio (80) of the PZT [14], (b) voltage waveform at the output of PZT. The switching frequency (56.1 kHz) was slightly higher than the frequency of resonance of PZT (56 kHz). The impedance of the device is the lowest in the neighborhood of resonant frequency. Therefore only the fundamental frequency component can pass through the resonator as evident in Fig. 9b.

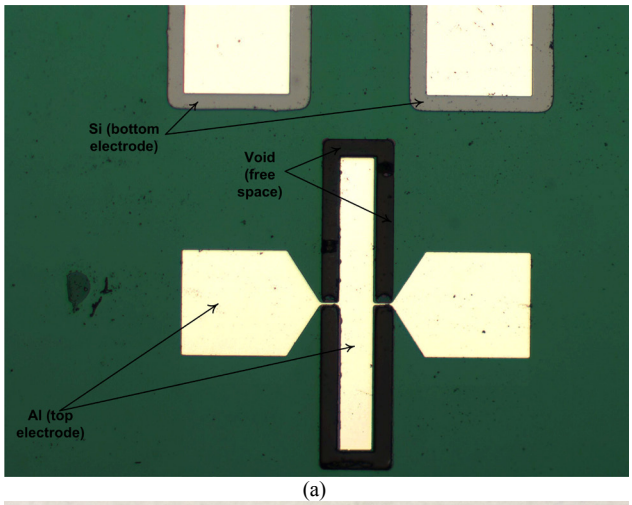

(a)

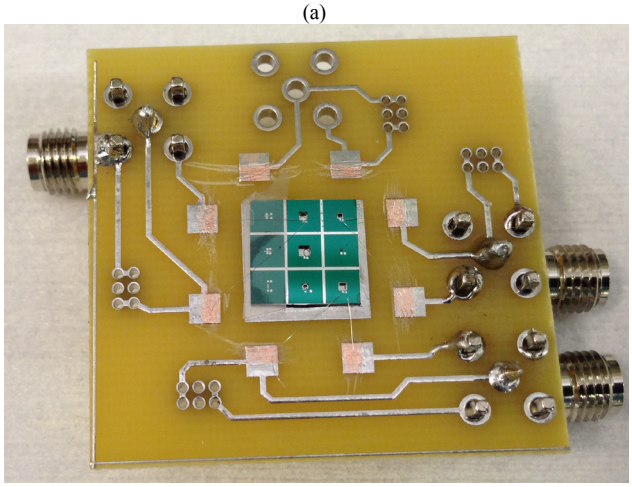

(b)

Fig. 10: (a) microscopic snapshot of the final device (10 times zoomed) (the green background is the 500 nm thick AlN piezoelectric film) (b) diced and packaged resonator on PCB for testing

anchor dimensions etc has not been optimized during the first run. As a result, the initial experimental results are not in good agreement with the simulation results. Fig. 10a shows the microscopic image of the final device. The post processed wafer was diced and the dies were glue to a PCB. The bond-pad of the devices was wire bonded to PCB pads for testing (Fig. 10b). A Vector network analyzer was used to get the S_{11} parameters of the device which was converted to impedance and phase (Fig. 11). The resonant frequency of the device was 183 MHz, which is quite high compared to the simulation results. Phosphoric acid at 100 ^{o}C etches Al at least five times faster than the AlN. The AlN layer was etched after depositing Al during the fabrication. This resulted in significant under etching of the Al top electrode, which in turn changed the device size in experimental prototype. This may be a reason for high resonant frequency in the prototype. The quality factor (QF) of the device is also low (~100), and non-optimized anchoring may lead to this low QF. Very thick bottom electrode (9 µm) compared to that of piezoelectric film (500 nm) may be another reason for

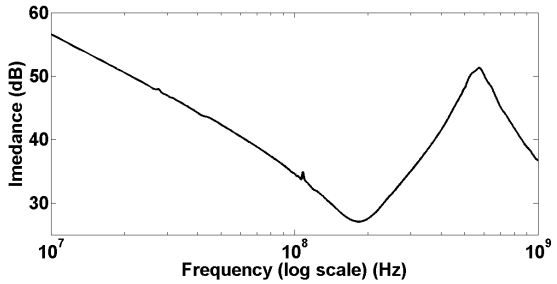

(a)

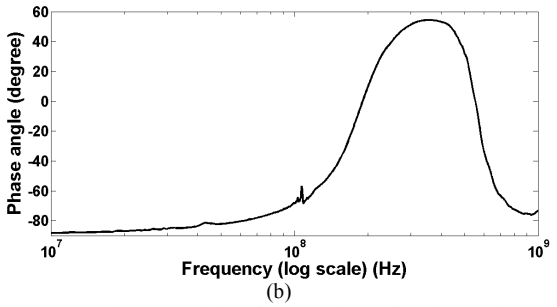

(b)

Fig 11 (a) Impedance, and (b) phase angle of the fabricated resonator with respect to frequency. The impedance is the lowest at the resonant frequency (183 MHz) where the resonator behaves like a resistor. Low Q of the resonator is evident from the absence of sharp peak at the frequency of resonance.

low QF. Authors are working on solving these issues for the future process runs.

VIII. Conclusions and Future Work

In this paper, a contour mode MEMS resonator has been presented with COMSOL Multiphysics simulation results of the device, and this resonator can be extended to build a MEMS transformer. TEG can convert the thermal energy from a human body to electricity, and the piezoelectric transformer based resonant converter can be used to harvest energy from such a small energy harvesting system. PSIM simulation results have been provided to prove this concept. Fabrication of the proposed device was carried out, and test results have been included in the paper. Authors are presently trying to fine tune the proposed process, and the existing limitations of the fabricated device will be addressed on future process runs. In addition, authors are involved in developing suitable resonant converter topologies to accommodate this proposed device for biomedical applications.

References

[1] A. M. Imtiaz, F. H. Khan, "Film bulk acoustic resonator (FBAR) based power converters: a new trend featuring EMI reduction and high power density," accepted at IEEE Applied Power Electronics Conference and Exposition (APEC), March 2013.

[2] G. Piazza, "Piezoelectric aluminum nitride RF MEMS for radio frequency front end technology," Ph.D dissertation, Univ. Calif., Berkeley, 2005.

[3] P. Osbond, C. M. Beck, C. J. Brierley, M. R. Cox, S. P. Marsh, N. M. Shorrocks, " The influence of ZnO and elelctrode thickness on the performance of thin film bulkacoustic resonators,"

[4] R. Ruby, " A decade of FBAR success and what is needed for another successful decade," Symposium on piezoelectricity, acoustic waves and device application (SPAWDA), pp. 365-369. 2011.

[5] Y. K. Ramadass, A. P. Chandrakasan, “A battery less thermoelectric energy harvesting interface circuit with 35 mV startup voltage,” IEEE Jour. Solid State Circuits, vol. 46, no. 1, Jan. 2011.

[6] E. J. Carlson, K. Strunz, B. P. Otis, “ A 20 mV input boost converter with efficient digital control for thermoelectric energy harvesting,” IEEE Jour. of Solid State Circuits, vol. 45, no. 4, April 2010.

[7] J. Kim, C. Kim, “ A DC-DC boost converter with variation tolerent MPPT technique and efficient ZCS circuit for thermoelectric energy harvesting,” IEEE Tran. Power Elec., vol. 28, no. 3, Aug. 2013.

[8] C. Y. Lin, “Design and analysis of piezoelectric transformer converters,” Ph. D dissertation, Virginia Tech, July, 1997.

[9] S. W. Tehon, “Piezoelectric and magnetostrictive transducers,” Ph. D. Dissertation, University of Illinois, Illinois, 1958.

[10] C. A. Rosen, “Analysis and design of ceramic transformer and filter elements,” PhD Dissertation, Syracuse University, Aug. 1956.

[11] P. Csavinszky, N. G. Einspruch, “ Effect of doping on the elastic constants of silicon,” Physical review letters, vol. 132, no. 6, pp. 2434-2440, 1963.

[12] A. K. Samaro, and F. Ayazi, “ Temperature compensation of silicon resonators via degenerate doping,” IEEE Tran. On Elec. Devices, vol. 59, no. 1, Jan. 2012, pp. 87-93.

[13] H. Fatemi, R. Abdolvand, “High frequency thin film piezoelectric transformers,” IEEE Int. Freq. Cont. Symp. Pp. 1-4, 2012.

[14] http://www.steminc.com/index.asp

[15] http://www.ultrasil.com

[16] http://www.oemgroupinc.com/foundry.php